View metadata, citation and similar papers at core.ac.uk
brought to you by CORE
provided by UCL Discovery

Electron confinement at diffuse ZnMgO/ZnO interfaces

Maddison L. Coke, Oscar W. Kennedy, James T. Sagar, and Paul A. Warburton

Citation: APL Mater. **5**, 016102 (2017); doi: 10.1063/1.4973669
View online: http://dx.doi.org/10.1063/1.4973669
View Table of Contents: http://aip.scitation.org/toc/apm/5/1
Published by the American Institute of Physics

Articles you may be interested in

Electronic structure of buried LaNiO3 layers in (111)-oriented LaNiO3/LaMnO3 superlattices probed by soft x-ray ARPES
APL Mater. **5**, 016101016101 (2017); 10.1063/1.4973558

Tuning of perovskite solar cell performance via low-temperature brookite scaffolds surface modifications
APL Mater. **5**, 016103016103 (2017); 10.1063/1.4973892

Laser-induced fluorescence analysis of plasmas for epitaxial growth of YBiO3 films with pulsed laser deposition
APL Mater. **4**, 126102126102 (2016); 10.1063/1.4971349

High ionic conductivity in confined bismuth oxide-based heterostructures
APL Mater. **4**, 121101121101 (2016); 10.1063/1.4971801

Running in circles looking for the best **science job?**
Search hundreds of exciting new jobs each month!
PHYSICS TODAY | JOBS
www.physicstoday.org/jobs

Electron confinement at diffuse ZnMgO/ZnO interfaces

Maddison L. Coke,[1] Oscar W. Kennedy,[1] James T. Sagar,[1]
and Paul A. Warburton[1,2]
[1]*London Centre for Nanotechnology, University College London, 17-19 Gordon Street, London WC1H 0AH, United Kingdom*
[2]*Department of Electronic and Electrical Engineering, University College London, Torrington Place, London WC1E 7JE, United Kingdom*

(Received 28 September 2016; accepted 21 December 2016; published online 10 January 2017)

Abrupt interfaces between ZnMgO and ZnO are strained due to lattice mismatch. This strain is relaxed if there is a gradual incorporation of Mg during growth, resulting in a diffuse interface. This strain relaxation is however accompanied by reduced confinement and enhanced Mg-ion scattering of the confined electrons at the interface. Here we experimentally study the electronic transport properties of the diffuse heteroepitaxial interface between single-crystal ZnO and ZnMgO films grown by molecular-beam epitaxy. The spatial extent of the interface region is controlled during growth by varying the zinc flux. We show that, as the spatial extent of the graded interface is reduced, the enhancement of electron mobility due to electron confinement more than compensates for any suppression of mobility due to increased strain. Furthermore, we determine the extent to which scattering of impurities in the ZnO substrate limits the electron mobility in diffuse ZnMgO–ZnO interfaces. © *2017 Author(s). All article content, except where otherwise noted, is licensed under a Creative Commons Attribution (CC BY) license (http://creativecommons.org/licenses/by/4.0/).* [http://dx.doi.org/10.1063/1.4973669]

ZnO has attracted much interest recently owing to its favourable electronic properties. ZnO is a wide band gap (3.37 eV) semiconductor[1] with a polar unit cell.[2] In ZnMgO, both the band gap and polarization depend upon the Mg concentration, x. At the interface between ZnO and ZnMgO, a combination of band-gap and polarization mismatch confines electrons to a two-dimensional electron gas (2DEG) with low-temperature electron mobility exceeding 10^6 cm^2 V^{-1} s^{-1}.[3] Such high mobilities have been realized due to high-quality interfaces made possible by molecular beam epitaxy (MBE) growth techniques. Mg incorporation also causes the c-lattice parameter of ZnMgO to decrease with increasing x due to the smaller atomic radius of Mg.[4] This is accompanied by a small increase in the a-lattice parameter.[5] Therefore, at an abrupt ZnO/ZnMgO interface some strain is inevitable. The strain can be relaxed if the system is in equilibrium during growth. This occurs through a redistribution of the Mg atoms across the interface region during the growth process, resulting in a less abrupt interface. Neighbouring unit cells have a small difference in Mg concentration and thus the lattice mismatch is negligible. By contrast, at abrupt interfaces, neighbouring unit cells have different lattice parameters, resulting in a significantly strained interface.

In order to create a high mobility 2DEG, it is necessary to minimize the amount of scattering. Scattering may occur both due to crystal defects associated with lattice mismatch between film and substrate and due to randomly substituted Mg atoms. At a diffuse interface we expect less scattering at the interface due to the more gradual release of strain, but an increase in random alloy scattering by comparison with abrupt interfaces. These two scattering mechanisms vary in importance depending on the spatial extent of the Mg redistribution at the interface. In addition, the degree of electron confinement depends upon the abruptness of the interface.

Here, we present an experimental study of the competing effects of electron scattering and confinement at ZnO/ZnMgO interfaces as we vary the spatial extent of the interface region. The Mg concentration gradient is controlled by varying the zinc flux during MBE growth and measured by x-ray photoelectron spectroscopy (XPS) depth-profiling. The electron mobility at the interface is extracted from magnetoresistance measurements at low temperature.

 © Author(s) 2017

We first calculate the band structure and electron concentration at a diffuse interface between two semi-infinite regions of ZnO and ZnMgO with growth direction [0001]. The region $z < 0$ is ZnO while the interface region $0 < z < \zeta$ is ZnMgO with the Mg content x being linearly graded from zero to x_0. The region $z > \zeta$ is uniformly ZnMgO with $x = x_0$. Hence, the diffuse interface extends from $z = 0$ to $z = \zeta$, the Mg concentration gradient in this region being $dx/dz = x_0/\zeta$, as shown in Figure 1(a). Band bending at the interface arises from two distinct sources—the spatial variation of both the bandgap and the polarization P. Specifically, the Maxwell-Gauss law states that the charge density ρ_{pol} arising from the polarization gradient is given by the divergence of P. In the absence of any polarization gradient, the carriers would be confined in the material with the lower bandgap as for a conventional GaAs–AlGaAs heterostructure. For a non-zero polarization gradient, however, it is possible for carriers to be confined in the interface region where the bandgap is not at its minimum value. This is schematically illustrated in Figure 1(a).

Furthermore, in Figures 1(b)–1(c), we present the results of self-consistent finite element simulations of ZnO/ZnMgO interfaces performed by solving the Poisson-Schrödinger equation. The equation is solved in one dimension with an element size of 1 Å.[1,6–10] The “bulk” Mg concentration at $z > \zeta$ is 40%. The carrier concentration in both the ZnMgO and ZnO far from the interface region is taken to be 10^{18} cm^{-3}.[11] This yields a sheet carrier concentration at the interface of 6.3×10^{12} cm^{-2}, this being independent of the width ζ of the interface region. At the abrupt interface ($dx/dz \rightarrow \infty$) a sharp, deep quantum well forms in the conduction band.[18] A 2DEG is formed at the surface of the ZnO. By contrast, for diffuse interfaces we see broader conduction band wells with the charge-confined region extending over the whole width of the interface region. This has previously been referred to as a three dimensional electron slab (3DES) and experimentally observed in ZnO/ZnMgO[12] and other polar materials such as AlGaN/GaN.[13] It results from the continuously spatially varying lattice parameter which gives rise to a continuously changing polarization. This leads to a built-in electric field across the interface. Free charges move into the ZnMgO layer in order to compensate for the built-in field, resulting in a lower carrier density than for the abrupt interface. This type of 3DES can only exist in crystal systems where polarization engineering is possible. For diffuse interfaces, a significant fraction of the carriers are located in the ZnMgO layer, unlike for abrupt interfaces. For $dx/dz = 1\%$ nm^{-1}, for example, 96% of the carriers are located in the interface region $0 < \zeta < z$.

ZnMgO films were grown directly onto Zn-polar ZnO polished substrates (SurfaceNet GmbH) in an MBE chamber at 750 °C for 1 h. Oxygen plasma was generated using a 300 W RF generator. The Zn beam equivalent pressure was measured by a retractable beam flux monitor. The elemental

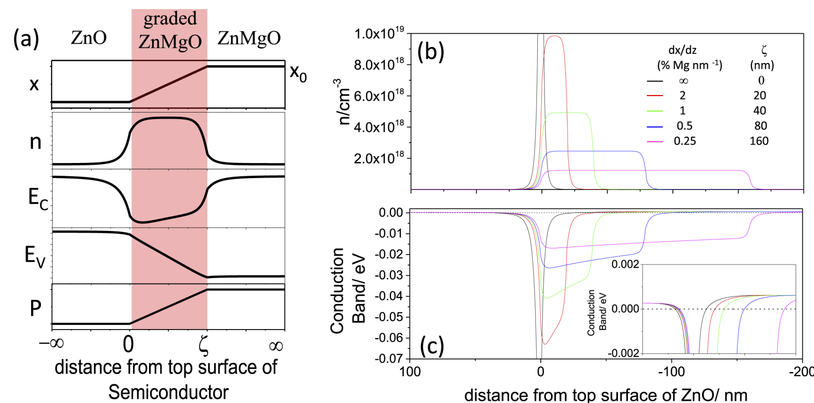

FIG. 1. (a) Schematic diagrams showing the fractional Mg concentration, x, carrier density, n, conduction band edge, E_C, valence band edge, E_V, and charge polarization, P, across a linearly graded interface of width ζ between ZnO and ZnMgO. Note that in reality the magnitude of the change in E_V exceeds that of E_C by one or two orders of magnitude so that the spatial variation of the bandgap essentially follows that of E_V. Self-consistent calculations of (b) the free electron density and (c) the conduction band offset, with the dotted line showing the Fermi energy, for selected values of the Mg concentration gradient, dx/dz, in the interface region. The “bulk” Mg concentration for $z > \zeta$ is x_0 = 40% in all cases. The inset in (c) shows the conduction band offset between ZnMgO and ZnO at a magnified scale.

composition was determined by XPS. A depth profile of the composition was obtained by sequential 3 keV argon-ion milling to a depth of 10 nm per iteration before performing *in situ* XPS measurements. X-ray diffraction (XRD) was used to characterize crystalline quality. Devices were fabricated by argon milling a mesa in the Hall bar geometry and sputtering Ti/Au (15 nm/50 nm) contacts. Resistivity and magnetoresistance measurements were carried out using a Quantum Design PPMS, in a perpendicular magnetic field.

In order to investigate the effect of varying the Mg gradient at the ZnO/ZnMgO interface, we must be able to control the Mg concentration gradient at the point of growth. The Mg gradient depends on the rate of Mg incorporation relative to the growth rate. This can be controlled by adjusting the zinc flux. With low Zn flux, re-evaporation and surface migration allow the system to reach equilibrium. The film becomes lattice latched[14] whereby the Mg content is determined by the excess energy the system has compared to that needed to grow a lattice mismatched unit cell. Conversely, at high Zn flux, due to the system not reaching equilibrium, a more abrupt Mg interface is grown.

In Figure 2(a) we show the spatial variation of the Mg content of five ZnMgO films grown at various values of Zn flux. We extract the Mg concentration gradient, dx/dz, by fitting to the approximately linear region of the depth profile close to the interface. The dependence of the Mg gradient upon the zinc flux for all samples is shown in Figure 2(b), confirming that more abrupt interfaces are obtained at higher zinc flux. Furthermore, at high zinc flux we can reduce the abruptness of the interface by increasing the temperature of the substrate (data not shown). This results from an increase in re-evaporation which reduces the growth rate, further confirming the above conjecture. The scatter in the data at low zinc flux is possibly due to variations in the substrate quality at the surface and mechanical polishing defects.

We now determine the crystallographic properties of the ZnMgO films using XRD. In order to analyse the interface strain we plot reciprocal space maps (RSMs) of two representative films, with Mg concentration gradients of 0.2% nm^{-1} (Figure 3(a)) and 1% nm^{-1} (Figure 3(b)). In both RSMs the high intensity central point is the $(01\bar{1}4)$ peak from the bulk ZnO substrate. Both RSMs show an additional peak which is caused by diffraction from the $(01\bar{1}4)$ ZnMgO planes. For the interface with the lower Mg gradient (Figure 3(a)), this peak is shifted with respect to the substrate peak in both Q_x and Q_z, showing that the ZnMgO lattice parameter has changed both in-plane and out of plane with respect to ZnO. For the more abrupt interface (Figure 3(b)), however, there is no shift in Q_x for the $(01\bar{1}4)$ ZnMgO peak, showing that the in-plane lattice parameter of the ZnMgO layer is the same as the underlying ZnO substrate. This film is therefore subject to in-plane strain. To maintain the ZnMgO unit cell volume, the shift in Q_z is larger for the more abrupt interface.

We now consider the electronic properties of the interfaces. We select five films, all of which have a maximum Mg concentration between 30% and 40%. The XPS depth profiles of these films are shown in Figure 2(a). The spatial extent of the interface region varies from 100 nm (corresponding to the whole grown film) to 40 nm. All five films show Shubnikov de Haas (SdH) oscillations at low temperatures in a perpendicular magnetic field. A typical magnetoresistance plot is shown in the inset

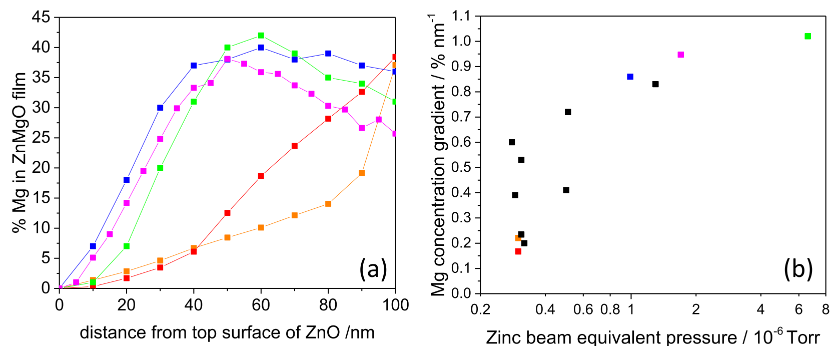

FIG. 2. (a) Mg concentration variation in five ZnMgO films as determined by XPS depth profiling. (b) Dependence of the interface Mg concentration gradient on the zinc beam-equivalent-pressure during MBE growth of the ZnMgO films. Coloured symbols in (b) correspond to the coloured plots in (a).

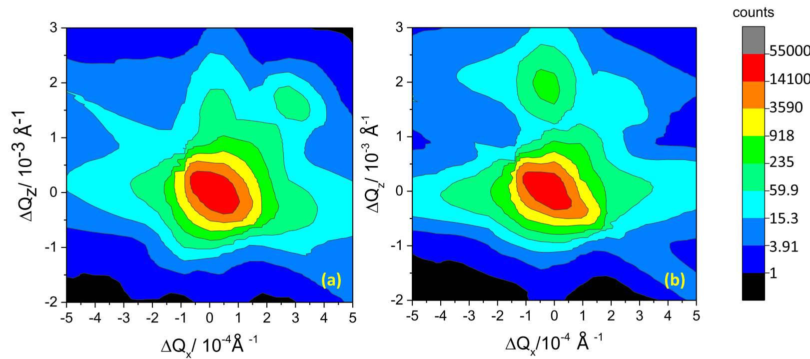

FIG. 3. X-ray diffraction reciprocal space maps referred to the $(01\bar{1}4)$ ZnO reflection in films with (a) an Mg concentration gradient of 0.2% nm^{-1} and (b) a higher Mg gradient of 1% nm^{-1}.

of Figure 4(a). At low field, prior to the onset of the SdH oscillations there is a region of negative magnetoresistance arising from the suppression of weak localization. The sheet carrier concentration extracted from the periodicity of the SdH plots is 3×10^{12} cm^{-2} with a sample-to-sample variation of ±25%. This value is consistent with those determined using the Poisson–Schrodinger model as shown in Figure 1(b). From the sheet carrier concentration the mobility can be extracted. This is shown as a function of the Mg interface concentration gradient in Figure 4(a). The mobility at 2 K is observed to be as high as 3100 cm^2 V^{-1} s^{-1}. This is two orders of magnitude higher than the low temperature mobility of ZnO,[15] confirming that substrate conduction plays no significant role. We also performed measurements of the Hall mobility which yield values within 10% of those in Figure 4(a), giving further confirmation that any parallel conduction paths are frozen out. Figure 4(a) shows a possible trend towards higher electron mobility for more abrupt interfaces, suggesting that, at least within the presented range of values of the Mg concentration gradient, the benefits of carrier confinement outweigh the additional scattering resulting from the strained lattice. This is the main conclusion of our experiments.

We note however that there is significant scatter in the data. Electron mobilities at ZnO/ZnMgO interfaces depend upon impurities in the substrates. The presence of residual lithium ions in the substrate can severely reduce the 3DES mobility.[16] Since the zero-field room-temperature electrical resistance of the substrate correlates with the residual lithium concentration,[17] we have plotted the dependence of the low temperature (i.e., confined electron dominated) mobility as a function of the room-temperature (i.e., substrate-conduction dominated) resistance as shown in Figure 4(b). The room-temperature resistance is measured through the same contacts used for the low temperature transport measurements. These are configured in a geometry which is not designed for and hence does not enable the extraction of the substrate resistivity. We observe that the data fall into two distinct

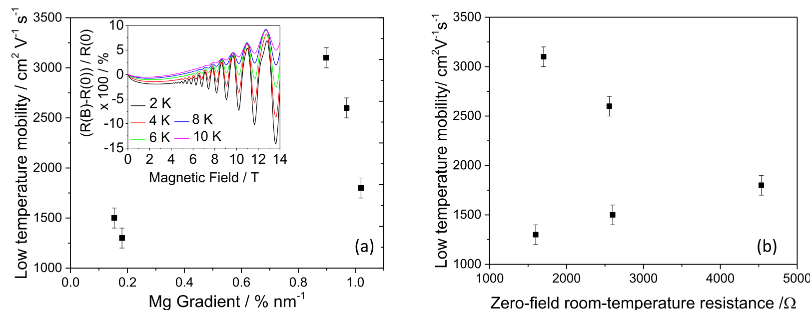

FIG. 4. (a) The electron mobility at $T = 2$ K (extracted from magnetoresistance measurements) as a function of the Mg concentration gradient dx/dz for films with bulk Mg content $x_0 = 40\%$. The inset is a typical magnetoresistance measurement showing SdH oscillations at various indicated temperatures. This film has $dx/dz = 1\%$ nm^{-1}. (b) Dependence of mobility at 2 K on zero-field room temperature substrate resistance.

sets. Films with less abrupt interfaces ($dx/dz \sim 0.2\%\ nm^{-1}$) have mobility less than 1600 $cm^2\ V^{-1}\ s^{-1}$ with no discernible dependence on the crystalline quality of the substrate. By contrast, films with more abrupt interfaces ($dx/dz \sim 1\%\ nm^{-1}$) show a marked increase in low temperature mobility as the room temperature resistance decreases. From these data we conclude that there exists a threshold level of electron confinement (corresponding to an Mg concentration gradient lying between 0.2% and 1% nm^{-1}), below which the mobility is limited by scattering off the Mg ions and above which it is limited by scattering off defects in the ZnO substrate.

We have demonstrated control over abruptness of ZnO/ZnMgO interfaces through the control of the Zn flux during growth. Varying the Mg concentration gradient affects both the electrostatics and the crystallographic strain at the interface. Although a more diffuse interface yields a more relaxed film with fewer crystalline defects, the electrons are confined in a region with a larger average Mg concentration. The electron mobility is reduced due to the increase in electron-ion scattering. The films with a larger Mg gradient are more strained yet see less Mg resulting in higher values of mobility. We conclude that degree of electron confinement in the graded system has a greater impact on the mobility than crystal defects induced by strain.

This work was supported by UK EPSRC Grant Reference No. EP/H005544/1 and by U.S. AFOSR Grant Reference No. FA8655-12-1-2126.

[1] A. Janotti and C. G. Van de Walle, "Fundamentals of zinc oxide as a semiconductor," Rep. Prog. Phys. **72**(12), 126501 (2009).
[2] H. Morkoç and Ü. Özgür, *General Properties of ZnO, in Zinc Oxide* (Wiley-VCH Verlag GmbH & Co. KGaA., 2009), pp. 1–76.
[3] J. Falson *et al.*, "MgZnO/ZnO heterostructures with electron mobility exceeding 1×10^6 cm^2/Vs," Sci. Rep. **6**, 26598 (2016).
[4] T. A. Wassner *et al.*, "Optical properties and structural characteristics of ZnMgO grown by plasma assisted molecular beam epitaxy," J. Appl. Phys. **105**(2), 023505 (2009).
[5] A. Ohtomo *et al.*, "$Mg_xZn_{1-x}O$ as a II–VI widegap semiconductor alloy," Appl. Phys. Lett. **72**(19), 2466–2468 (1998).
[6] Y. Kozuka *et al.*, "Precise calibration of Mg concentration in $Mg_xZn_{1-x}O$ thin films grown on ZnO substrates," J. Appl. Phys. **112**(4), 043515 (2012).
[7] A. Malashevich and D. Vanderbilt, "First-principles study of polarization in $Zn_{1-x}Mg_xO$," Phys. Rev. B **75**(4), 045106 (2007).
[8] H. Tampo *et al.*, "Band profiles of ZnMgO/ZnO heterostructures confirmed by Kelvin probe force microscopy," Appl. Phys. Lett. **94**(24), 242107 (2009).
[9] G. L. Snider, I. H. Tan, and E. L. Hu, "Electron states in mesa-etched one-dimensional quantum well wires," J. Appl. Phys. **68**(6), 2849–2853 (1990).
[10] I. H. Tan *et al.*, "A self-consistent solution of Schrödinger–Poisson equations using a nonuniform mesh," J. Appl. Phys. **68**(8), 4071–4076 (1990).
[11] N. A. Jayah *et al.*, "High electron mobility and low carrier concentration of hydrothermally grown ZnO thin films on seeded a-plane sapphire at low temperature," Nanoscale Res. Lett. **10**(1), 7 (2015).
[12] J. Ye *et al.*, "Spin-polarized wide electron slabs in functionally graded polar oxide heterostructures," Sci. Rep. **2**, 533 (2012).
[13] D. Jena *et al.*, "Realization of wide electron slabs by polarization bulk doping in graded III–V nitride semiconductor alloys," Appl. Phys. Lett. **81**(23), 4395–4397 (2002).
[14] M.delP. Rodríguez-Torres *et al.*, "Investigation of the 'composition-pulling or lattice-latching' effect in LPE," J. Cryst. Growth **277**(1–4), 138–142 (2005).
[15] P. Wagner and R. Helbig, "Halleffekt und anisotropie der beweglichkeit der elektronen in ZnO," J. Phys. Chem. Solids **35**(3), 327–335 (1974).
[16] P. T. Neuvonen *et al.*, "Intrinsic point-defect balance in self-ion-implanted ZnO," Phys. Rev. Lett. **110**(1), 015501 (2013).
[17] E. D. Kolb and R. A. Laudise, "Hydrothermally grown ZnO crystals of low and intermediate resistivity," J. Am. Ceram. Soc. **49**(6), 302–305 (1966).
[18] In reality, due to the finite element size used, the curves labelled $dx/dz \to \infty$ correspond to a change in Mg concentration from zero to 40% over one element, i.e., $dx/dz = 400\%\ nm^{-1}$.